

# The Discovery of $\lambda$ Bootis Stars – The Southern Survey II

Simon J. Murphy<sup>1,2\*</sup>, Richard O. Gray<sup>3</sup>, Christopher J. Corbally<sup>4</sup>,

Charles Kuehn<sup>1,5</sup> Timothy R. Bedding<sup>1,2</sup> and Josiah Killam<sup>3</sup>

<sup>1</sup> *Sydney Institute for Astronomy (SfA), School of Physics, University of Sydney, NSW 2006, Australia*

<sup>2</sup> *Stellar Astrophysics Centre, Department of Physics and Astronomy, Aarhus University, 8000 Aarhus C, Denmark*

<sup>3</sup> *Department of Physics and Astronomy, Appalachian State University, Boone, NC 26808, USA*

<sup>4</sup> *Vatican Observatory Research Group, Steward Observatory, Tucson, AZ, 85721-0065 USA*

<sup>5</sup> *Department of Physics and Astronomy, University of Northern Colorado, Greeley, CO 80639, USA*

Accepted XXX. Received YYY; in original form ZZZ

## ABSTRACT

The  $\lambda$  Boo stars are chemically peculiar A-type stars whose abundance anomalies are associated with the accretion of metal-poor material. We searched for  $\lambda$  Boo stars in the southern hemisphere in a targeted spectroscopic survey of metal-weak and emission-line stars. Obtaining spectra for 308 stars and classifying them on the MK system, we found or co-discovered 24 new  $\lambda$  Boo stars. We also revised the classifications of 11 known  $\lambda$  Boo stars, one of which turned out to be a chemically normal rapid rotator. We show that stars previously classified in the literature as blue horizontal branch stars or emission-line A stars have a high probability of being  $\lambda$  Boo stars, although this conclusion is based on small-number statistics. Using WISE infrared fluxes, we searched our targets for infrared excesses that might be attributable to protoplanetary or debris discs as the source of the accreted material. Of the 34  $\lambda$  Boo stars in our sample, 21 at various main-sequence ages have infrared excesses, confirming that not all  $\lambda$  Boo stars are young.

**Key words:** stars: chemically peculiar – stars: circumstellar matter – stars: emission-line, Be – stars: early-type – stars: evolution

## 1 INTRODUCTION

Long-standing puzzles in astrophysics often contain clues on physics that is missing from stellar models. The  $\lambda$  Boo stars are one such puzzle. They are chemically peculiar A or F-types stars first identified as a distinct class in the 1950s (Slettebak 1952, 1954), and a complete explanation for their peculiarity is still lacking despite recent efforts (Jura 2015; Kama et al. 2015; Jermyn & Kama 2018). They are characterised by metal weaknesses with a specific chemical abundance profile. Refractory elements such as magnesium and iron-peak elements are underabundant by  $-0.5$  to  $-2.0$  dex (Andrievsky et al. 2002) while volatile elements such as carbon, nitrogen, and oxygen have near-solar abundances (Baschek & Slettebak 1988; Kamp et al. 2001; Folsom et al. 2012).

The abundance dichotomy between refractories and volatiles suggests that accretion from a circumstellar disc

plays a role in the development or maintenance of the chemical anomalies (Venn & Lambert 1990; Turcotte & Charbonneau 1993; King 1994). The material itself does not need to be metal-weak because a variety of efficient dust-gas separation mechanisms can operate around A stars (Jermyn & Kama 2018), allowing volatile-rich gas to be accreted onto the star without the refractory dust (Waters et al. 1992). Suggestions for the accretion source have included material left-over from star formation (Holweber & Sturenburg 1993), gas from dense regions of the ISM (Kamp & Paunzen 2002), and material ablated from hot jupiters (Jura 2015). Protoplanetary discs are particularly likely sources, especially since embedded planets can deplete the dust in a way that reproduces observed  $\lambda$  Boo abundances (Kama et al. 2015; Jermyn & Kama 2018). VLTI and ALMA observations confirm the existence of planets embedded in the discs of some  $\lambda$  Boo stars (e.g. Matter et al. 2016; Fedele et al. 2017; Cugno et al. 2019; Toci et al. 2020).

Numerical calculations have shown that peculiarities from selective accretion ought to persist for only  $10^6$  yr once

\* E-mail: simon.murphy@sydney.edu.au (SJM)

accretion has stopped (Turcotte & Charbonneau 1993), before particle transport processes erase the chemical abundance signature. It then follows that most  $\lambda$  Boo stars should be actively accreting. However, Gray et al. (2017) found that  $\lambda$  Boo stars were no more likely to be observed with a debris disc at  $22\mu\text{m}$  than chemically normal A stars. It is also apparent that not all  $\lambda$  Boo stars are young: they are found at a wide range of main-sequence ages when placed on an HR diagram, according to either their spectroscopic  $\log g$  values (Iliev & Barzova 1995) or luminosities derived from precise *Gaia* parallaxes (Murphy & Paunzen 2017).

The age range of  $\lambda$  Boo stars suggests a reservoir of material may be needed from which the star can accrete at an arbitrary age. Such a reservoir may include comets, such as the 400-Earth-mass cloud of CO-rich comets postulated to orbit the A stars HD 21997 and 49 Ceti (Zuckerman & Song 2012). So-called ‘swarms’ of comets, not unlike the fragmented comet Shoemaker–Levy 9 that delivered large quantities of volatiles to Jupiter (Lellouch et al. 1997), have been used to explain the peculiar transits of the *Kepler* A star KIC 8462852 (Boyajian et al. 2016; Bodman & Quillen 2016). Such bodies, sometimes called Falling Evaporating Bodies (FEBs), may be perturbed from dormant orbits by mean-motion resonances with massive planets (Freistetter et al. 2007) or encounters with nearby stars (Bailer-Jones 2015; Gray et al. 2017). This comet-reservoir scenario has a pedigree in  $\beta$  Pic (King & Patten 1992; Gray & Corbally 2002), a planet-host with  $\lambda$  Boo-like properties (Lagrange et al. 2010; Cheng et al. 2016; Snellen & Brown 2018), FEB-like spectral absorption signatures (Ferlet et al. 1987; Karmann et al. 2001; Thébault & Beust 2001; Karmann et al. 2003), and transiting exocomets (Zieba et al. 2019).

A solution to the  $\lambda$  Boo puzzle requires a broad approach, including particle transport models for stars and discs, and a larger and better characterised set of observations. To address the latter, Murphy et al. (2015) re-investigated all known and candidate  $\lambda$  Boo stars to create a homogeneous catalogue of class members, resulting in 64 bona-fide  $\lambda$  Boo stars and 45 candidates for which more observations are required for a definite classification. Since  $\lambda$  Boo stars are rare, with only 2% of A stars belonging in the class (Gray & Corbally 1998), further expansion of the membership list requires efficient target selection.

In Gray et al. (2017, Paper I, hereafter), we began a search for new  $\lambda$  Boo stars using GALEX photometry to target A stars with UV excesses. The  $\lambda$  Boo stars have reduced line blanketing in the UV because they are metal weak, and hence show UV excesses compared to normal stars. We found 33 new southern  $\lambda$  Boo stars and confirmed 12 others with that approach. By modelling their spectral energy distributions, we were also able to search for infrared excesses to make an unbiased assessment of the occurrence rate of discs around  $\lambda$  Boo stars, finding the aforementioned result that discs are no more likely around  $\lambda$  Boo stars at  $22\mu\text{m}$  than around normal stars.

This is the second paper in the series, also focussing on the southern hemisphere (declination  $< +15^\circ$ ). Observations of northern targets are ongoing and will be presented in future papers. In this paper, we particularly target known emission-line stars. Folsom et al. (2012) observed that many emission-line A stars were also  $\lambda$  Boo stars – an observation compatible with the hypothesis that  $\lambda$  Boo stars are

active accretors. In addition to the emission-line stars, we created a target list of metal-weak objects by examining their Strömgren photometry. Our target selection, observations, and spectral classification procedures are described in Sec. 2.

We also look for infrared excesses around our targets, which might indicate the source of the accreted material if the accretion episode is recent or ongoing. We describe our SED modelling and search for infrared excesses in Sec. 3, and present conclusions in Sec. 4.

## 2 METHOD

### 2.1 Sample selection

To improve the success rate of searching for  $\lambda$  Boo stars beyond the 2% one expects at random, we compiled a target list from several types of stars that we considered likely to yield new  $\lambda$  Boo stars. Unlike Paper I, our goal was only to find more  $\lambda$  Boo stars, and although we didn’t specifically favour stars with infrared excesses, we did not actively eliminate such survey bias. A major focus in this work was emission-line A stars, but relatively few ( $<50$ ) of these are known. Blue horizontal branch (BHB) stars are another class of rare metal-weak A stars that we considered to be promising targets, since some might have been misclassified in the literature. The target list therefore contained a mixture of emission-line stars, BHB stars, and a large number of metal-poor stars selected using Strömgren photometry. Due to good weather and efficient observing, we added a further group of targets on the final night of the observing run, comprising A and early F stars observed in Campaign 01 of the K2 Mission. Targets were organised into groups based on how they were selected (see Table 1):

Group 0. *Known  $\lambda$  Boo stars.* In order to verify that the spectra were suitable for accurate classification, we obtained spectra of eleven known  $\lambda$  Boo stars, chosen according to availability on the sky at the time of observation. One of these, HD 111164, was classified as a  $\lambda$  Boo star by Abt & Morrell (1995), but turned out to be a chemically normal rapid rotator.

Group 1. *Emission-line A stars (i).* We used the criteria search function of the SIMBAD database (Wenger et al. 2000) to select spectral types matching “A[0-9]\*e”, where ‘[0-9]’ represents any integer in this range, the asterisk is a wildcard of any length, and ‘e’ is the standard notation for emission lines. These are Herbig Ae/Be stars (Herbig 1960; Hillenbrand et al. 1992), the hotter analogues of T Tauri stars (Joy 1945; Appenzeller & Mundt 1989). We expected that focussing on emission line stars would increase the efficiency of our  $\lambda$  Boo search by preferentially observing stars with circumstellar discs, or stars accreting material from an unknown source. Having a larger sample of such stars is also useful for ascertaining any link between age, accretion, and  $\lambda$  Boo peculiarity. Of the 308 stars observed, 20 stars came from this group.

Group 2. *Emission-line A stars (ii).* This group is phenomenologically identical to the previous group, except that the search terms were slightly modified to capture stars whose spectral types had been recorded differently. We searched for object types matching

“Em\*/Ae\*” and “spectral type = A”. Of the 308 stars observed, 18 stars came from this group.

Group 3. *Photometrically metal-weak stars*. Strömgren photometry can be used quite efficiently to select metal-weak stars from a sample of A stars. The  $m_1$  index is sensitive to metallicity, with metal-weak stars having lower values of  $m_1$  than normal stars at a given  $b - y$  colour (see Paunzen & Gray 1997). We selected stars using the following criteria:

- i.  $-0.015 < (b - y) < 0.30$
- ii.  $m_1 > 0.130 - 0.3(b - y)$
- iii.  $m_1 < 0.220 - 0.3(b - y)$
- iv.  $c_1 < 1.4 - 2.0(b - y)$

and prioritised targets with Tycho  $B$  magnitudes  $< 10$  that had not already been observed by Paunzen & Gray (1997) or other papers in that series (Paunzen et al. 2001; Paunzen 2001). Of the 308 stars observed, 210 stars came from this group.

Group 4. *Blue-horizontal-branch (BHB) stars*. At classification resolution ( $R \sim 3000$ ), the spectra of BHB stars are quite similar to  $\lambda$  Boo stars. We observed seven BHB stars from MacConnell et al. (1971) as a likely source of additional  $\lambda$  Boo stars.

Group K2. *Targets scheduled to be observed in Campaign 01 of the K2 Mission*. Space photometry can be beneficial to the study of  $\lambda$  Boo stars in multiple ways. For instance, there are  $\lambda$  Boo stars with exoplanets, such as HR 8799 (Soummer et al. 2011), so space photometry might reveal exoplanet (or exocomet) transits around  $\lambda$  Boo stars. In addition, the same photometry can be used for asteroseismology. Stellar oscillations are sensitive to metallicity, and can be used to determine whether stars are globally metal-poor or just have surface peculiarities (Murphy et al. 2013). We therefore observed some A-type stars that were scheduled to be observed in Campaign 01 of the K2 Mission (Howell et al. 2014). This group was not selected according to spectroscopic or photometric properties, so it is numbered differently from the others. It is also not anticipated to yield a higher number of  $\lambda$  Boo stars than the 2% expected from a random draw of field stars. Of the 308 stars observed, 42 stars came from this group, and we found one (HD 98069) to be a  $\lambda$  Boo star. Its K2 light curve reveals it is a  $\delta$  Sct star with eight pulsation peaks exceeding 1 mmag and a further seven exceeding 0.5 mmag, most of which lie between 12 and 18 d<sup>-1</sup>. Further asteroseismic analysis is beyond the scope of this work. A TESS light-curve is also available, has similar properties, and has been analysed along with the lightcurves of all southern  $\lambda$  Boo stars by Murphy et al. (2020).

Our target list reflects our single-site, single-epoch observations (Sec. 2.2): only targets observable during 2014 Mar were included, corresponding roughly to right ascension in the range 75–300°. Our focus on emission line stars (Groups 1 and 2) produced many new targets not already searched for  $\lambda$  Boo stars, whereas the Strömgren targets (Group 3) have an overlap of 21 targets with Paper I, which were observed at SAAO in 2013 and 2014. Some overlap is desirable to check for consistency between different instruments, noting of course that some targets may be spectrum variables. Because some of those 21 overlapping stars are  $\lambda$  Boo stars, they are co-discoveries. Two stars (HD 94326 and HD 102541) whose SAAO spectra showed  $\lambda$  Boo spec-

**Table 1.** Breakdown of the target selection groups described in Sec. 2.1, the number of stars in each group ultimately classified as  $\lambda$  Boo stars (including the two uncertain “ $\lambda$  Boo?” stars), the total number of targets in each group, and the percentage of  $\lambda$  Boo stars obtained by dividing the previous two columns.

Group	Description	Num. $\lambda$ Boo	Total	Percent
0	Known $\lambda$ Boo stars	10	11	91%
1	“A[0-9]*e”	4	20	20%
2	“Em*/Ae*” and “A”	1	18	6%
3	Photometrically met wk	16	210	8%
4	BHB stars	2	7	29%
K2	K2 targets	1	42	2%

tral features are classified as non- $\lambda$  Boo metal-weak stars in this work. More spectra and an abundance analysis are desirable to confirm whether these are indeed  $\lambda$  Boo stars, and to analyse the variability in their spectra. Other than the 21 overlapping targets and the 11 in Group 0, the remainder (276) were unique to this survey.

## 2.2 Observations

During 2014 Mar 17–19 we obtained spectra of 308 targets with the WiFeS spectrograph (Dopita et al. 2007) on the ANU 2.3-m telescope at Siding Spring Observatory. Our spectra were obtained in the blue-violet region in B3000 mode and have a resolution of about 2.5 Å/2 pixels. The WiFeS data were reduced with the PYWIFES software package (Childress et al. 2014). Due to difficulty in rectifying the spectra over the Balmer jump, we trimmed the spectra to the range 3865–4960 Å. The spectra thus cover the region between the blue wing of H $\delta$  and the red wing of H $\beta$ . The spectra are qualitatively similar to those made from SAAO for Paper I.

## 2.3 Spectral classification

We classified the spectra on the MK system, which is described by Gray & Corbally (2009). The  $\lambda$  Boo stars are described in detail there and in Paper I, so we give only a summary here. When classifying A stars, the three main temperature criteria are (i) the strength of the Ca II K line, which rapidly increases towards later (cooler) types; (ii) the strength of the Balmer lines of hydrogen, which have a broad maximum around A2 and decrease on either side; and (iii) the metal lines, which increase in strength almost uniformly from A0 to F0. Ordinarily, all of these are absorption lines and in a normal star, all three criteria would yield the same temperature subclass. This is not the case in the  $\lambda$  Boo stars, where the metal lines are weak for a given hydrogen line type. It is the hydrogen lines that give the best estimate of the true stellar temperature, hence the spectra are usually classified with their hydrogen line type, then the luminosity class, then the K and metal line types, e.g. A7 V kA2mA2  $\lambda$  Boo. Spectral types of  $\lambda$  Boo stars having only mild peculiarity are written with the class name in parentheses: “( $\lambda$  Boo)”. For F-type stars, the G-band becomes an important feature, and this is sometimes written prepended with a ‘g’, e.g. F5 V mF2gF5.

Each spectrum was classified by SJM and independently

by at least one other author (ROG or CJC), and without knowledge of which group the target originated from. Any spectrum for which the initial classifications were found to disagree was reclassified by all three classifiers and discussed until agreement was reached on the best-fitting spectral type. The spectral types of the targets are given in Table A1. For explanations of notation used in spectral classes, e.g. ‘e’ for emission and ‘s’ for sharp-lined, see Gray & Corbally (2009) and Smith et al. (2011).

### 3 STELLAR PARAMETERS AND INFRARED EXCESSES

Establishing the mechanisms that lead to  $\lambda$  Boo peculiarities requires a better understanding of the environments of the stars. In particular, the accretion of dust-depleted material requires a reservoir, whose thermal emission might be detectable above the stellar luminosity in the infrared. To search for this, we constructed spectral energy distributions (SEDs) of our targets using stellar atmosphere models, against which we compared infrared fluxes from 2MASS and WISE. We followed the method from Paper I, which is summarised in this section.

#### 3.1 Physical Parameters and Reddening

Stellar physical parameters were determined via  $\chi^2$  minimisation between the observed spectra and a library of synthetic spectra computed with SPECTRUM (Gray & Corbally 1994) and ATLAS9 (Castelli & Kurucz 2004). The library grid has effective temperatures spanning 6500–25 000 K (having 50-K spacing up to 10 000 K, then 100-K spacing to 11 500 K, 500-K spacing to 13 000 K, and 1000-K spacing to 25 000 K), with  $\log g = 3.3, 3.6, 4.0$ , and  $4.2$ , and with metallicities of  $[M/H] = +0.5, +0.2, 0.0, -0.2, -0.5, -1.0, -1.5$ , and  $-2.0$ . We used the stellar spectral types (see Sec. 2.3) to estimate the intrinsic  $(B - V)_0$  colours of the stars according to the relation in Paper I, making allowances for differences in stellar metallicity.

Photometric fluxes were downloaded from IPAC.<sup>1</sup> We used Johnson B and V; 2MASS J, H and K; and WISE W1, W2, W3 and W4. Reddening ( $E(B - V)$ ) was evaluated by comparing the observed  $B - V$  colours with our intrinsic  $(B - V)_0$  colours, and the infrared fluxes were dereddened with a combination of the Fitzpatrick reddening law (Fitzpatrick 1999) and the mid-infrared extinction law of Xue et al. (2016). When Johnson B and V were unavailable, we used Tycho  $B_T$  and  $V_T$  (Høg et al. 2000) instead and followed a similar reddening procedure with a slightly different relation (Paper I) to account for the difference in zero-points of the two photometric systems (Bessell & Murphy 2012).

#### 3.2 Infrared Excesses

We compared the W1, W2, W3 and W4 fluxes to the synthetic spectra to identify stars with infrared excesses. We normalised the spectra to the 2MASS J band, except where there were clear excesses in the 2MASS bands, in which

case spectra were normalised to the V band instead. We recorded infrared excesses (in W1–W4) in the form of a flux ratio,  $(F_{\text{obs}} - F_{\text{model}})/F_{\text{model}}$ , and calculated the significance of those excesses using the recorded errors for the WISE photometry. Following Paper I, we considered infrared excesses significant at  $2\sigma$  rather than the conventional  $3\sigma$ , to avoid missing potentially interesting targets for future follow-up. This is particularly important for the detection of cool discs that do not radiate strongly at wavelengths below  $22\ \mu\text{m}$  (i.e. WISE W4). Stars with excesses at  $\geq 2\sigma$  are indicated in Table A1, and the values and significances of the excesses are given in Table 2. SED parameters for stars without infrared excesses are given separately in Table 3.

We find that 21 of the 34  $\lambda$  Boo stars in our sample have IR excesses. Seven of them exceed  $10\sigma$  in strength, and six of those (HD 101412, HD 139614, HD 141569, HD 169142, NGC 6383 22, and T Ori) have excesses that are larger at longer wavelengths, suggesting circumstellar discs (Fig. 1). We found emission lines in the spectrum of HD 139614, which is known to be a pre-main sequence star with a protoplanetary disc (Matter et al. 2016; Carmona et al. 2017; Laws et al. 2020), in the less well-studied accretor HD 101412 (Cowley et al. 2012; Schöller et al. 2016), and in the cluster member T Ori. For HD 141569 and HD 169142, we found no emission in our spectra, even though HD 141569 is known to have a Kuiper-Belt-like debris disc (Mendigutía et al. 2017; Mawet et al. 2017; Miley et al. 2018; White et al. 2018; Bruzzone et al. 2020) and HD 169142 has a protoplanetary disc (Fedele et al. 2017; Carney et al. 2018; Ligi et al. 2018; Chen et al. 2019; Gratton et al. 2019; Macías et al. 2019; Toci et al. 2020). For NGC 6383 22, our spectrum shows weak emission. Further observations of this target would be worthwhile, especially high-resolution spectroscopy in the visible for an abundance analysis, and ALMA or VLT observations for dust characterisation. The seventh target with a  $>10\sigma$  IR excess is HD 314915. Although this is classified as an emission-line star on SIMBAD (from Nesterov et al. 1995), its SED appears to be more consistent with a cool binary companion (Fig. 2).

Table 4 shows the fraction of stars in each target selection group with infrared excesses. The K2 targets constitute the only group that is presumably unbiased with respect to infrared excess, and in that group, out of 41 normal A-type stars, 10 show excesses at  $\geq 2\sigma$  in one or more WISE bands. That is a proportion of  $24.4 \pm 7.7\%$ . In Paper I, 18 out of 121 normal A-type stars in the Tycho sample showed excesses, giving a proportion of  $14.9 \pm 3.5\%$ . According to a two-tailed Z test, the resulting z-score is 1.3225, with a p value of 0.187, so those two proportions are not significantly different. Combining the K2 and Tycho normal star samples, we find that out of a total of 162 normal A-type stars, 28 show WISE  $2\sigma$  excesses, or a proportion of  $17.3 \pm 3.3\%$ . This is similar to the  $20.0 \pm 10\%$  observed for  $\lambda$  Boo stars in Paper I, although a larger unbiased sample of  $\lambda$  Boo stars is clearly needed before we can make any meaningful statement about whether the proportion of  $\lambda$  Boo stars with IR excesses differs from that of normal A-type stars.

#### 3.3 Luminosities

To position the  $\lambda$  Boo stars in our sample on the HR diagram, we determined their luminosities. We followed the

<sup>1</sup> <https://irsa.ipac.caltech.edu/>



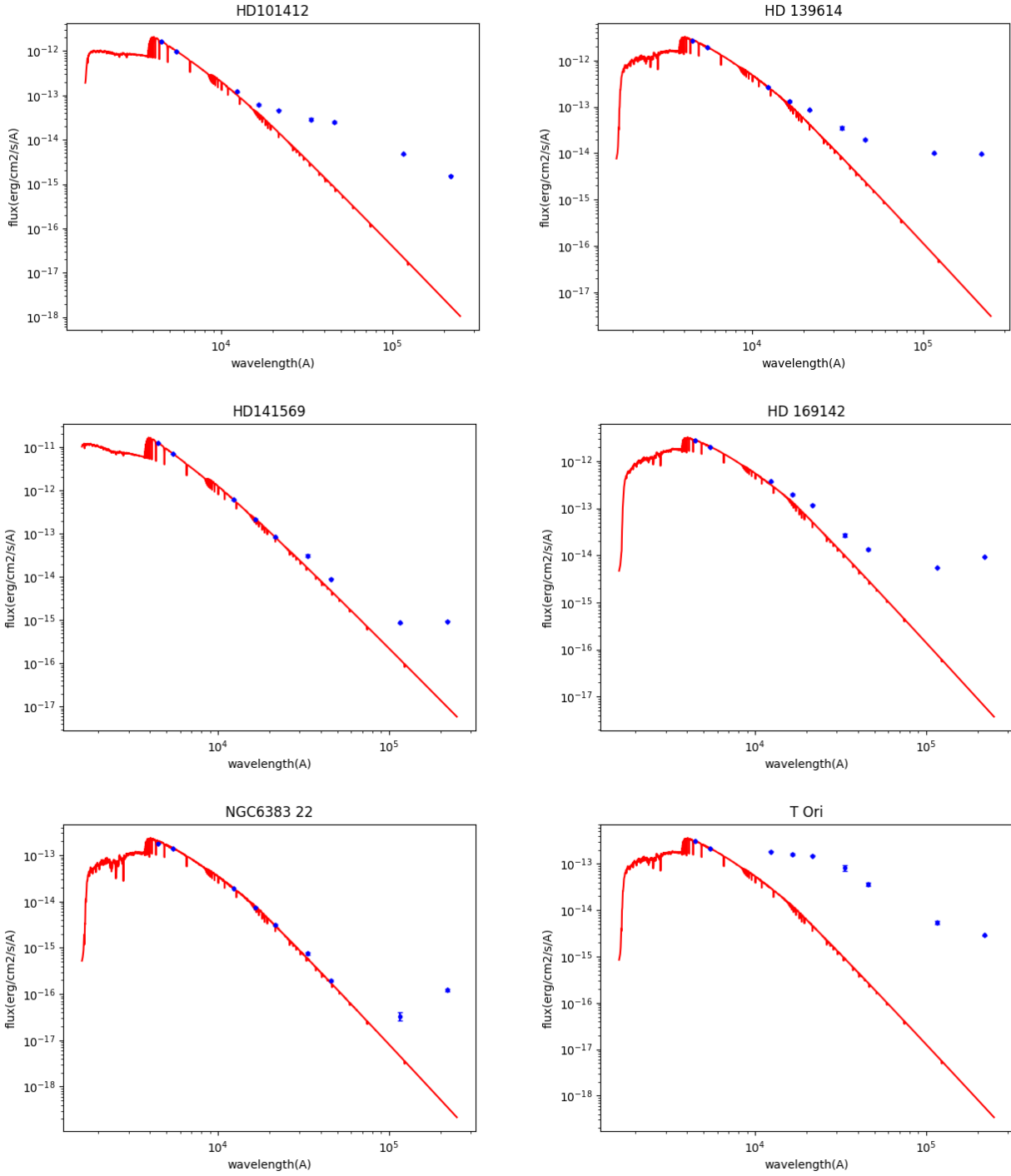


**Figure 1.** Spectral energy distributions (SEDs) for the six  $\lambda$  Boo stars with strong infrared excesses ( $>10\sigma$  in any of the WISE passbands) that probably originate from discs. Blue data points are photometric fluxes in Johnson B and V; 2MASS J, H and K; and WISE W1, W2, W3 and W4.

methodology of [Murphy et al. \(2019\)](#) and [Hey et al. \(2019\)](#), except that we used the Johnson V band rather than SDSS g. Bolometric luminosities were calculated via absolute magnitudes using standard formulae:

$$M_V = m_V - 5(\log d - 1) - A_V, \quad (1)$$

and

$$\log L_{\text{bol}}/L_{\odot} = -(M_V + BC - M_{\text{bol},\odot})/2.5. \quad (2)$$

The apparent V magnitudes,  $m_V$ , are those in Table A1, which are taken from the SIMBAD database with an assumed uncertainty of 0.02 mag. The V-band extinctions,  $A_V$ , were taken as  $3.1E(B - V)$ , using the  $E(B - V)$  values deter-

**Table 2.** Infrared excesses for all stars of the sample with a  $\geq 2\sigma$  excess in one or more WISE bands. Twelve rows are shown; the full table is available online in machine-readable format. Model parameters ( $T_{\text{eff}}$ ,  $\log g$ ,  $[\text{Fe}/\text{H}]$  and  $E(B-V)$ ) describe the spectral energy distributions, and asterisks in the  $T_{\text{eff}}$  column indicate the stars for which the  $V$  band rather than the  $J$  band was used for normalisation. Infrared excesses (“val.”) are given as the flux fraction in excess of the model, i.e.  $(F_{\text{obs}} - F_{\text{model}})/F_{\text{model}}$ .

Obj. Name	Spectral Type	$T_{\text{eff}}$	$\log g$	[Fe/H]	$E(B-V)$	W1		W2		W3		W4	
		K				mag	val.	$\sigma$	val.	$\sigma$	val.	$\sigma$	val.
BD-15 1548	B7 IIIe He-wk	13000 *	3.3	0.0	0.2	1.2	25.8	1.5	32.9	3.5	40.7	9.5	10.1
BD-15 4515	F2 V kA4mA6 $\lambda$ Boo	7000	4.2	-1.5	0.108	0.1	3.6	0.1	5.5	0.1	6.0	...	...
CD-37 3833	A2 Vn kA0	8700	4.2	-0.5	0.05	...	...	...	...	0.1	2.4	...	...
CD-48 3541	A2 Vn kA0mA1	8900 *	4.2	-1.0	0.04	...	...	...	...	0.1	2.1	1.5	2.7
CD-55 2595	B1 Ve	25000 *	4.0	0.0	0.31	0.3	12.1	0.6	20.9	1.4	19.9	...	...
CD-59 1764	A0.5 V	9650	4.2	0.0	0.052	...	...	...	...	0.1	3.4	1.0	2.1
CD-60 1932	A0 Vnn	9800	4.2	0.0	0.033	0.1	5.6	0.1	6.9	0.2	6.1	0.9	2.2
CD-60 4157	A1 Van	9500	4.2	0.0	0.162	...	...	...	...	...	...	1.0	3.3
CPD-58 3138	A1.5 Vs	9200	4.2	0.0	0.06	0.1	2.8	0.0	2.4	...	...	...	...
HD 100380	A4 IVs	8350	4.0	0.0	0.035	...	...	0.1	3.2	...	...	0.1	3.4
HD 100453	F1 Vn	7100 *	4.2	0.0	0.0	7.1	4.0	20.9	5.3	184.4	98.7	2283.8	136.2
HD 101412	A3 V(e) kA0.5mA0.5 ( $\lambda$ Boo)	8500 *	4.2	-1.5	0.114	9.2	16.0	28.6	18.0	208.8	108.6	888.1	90.9

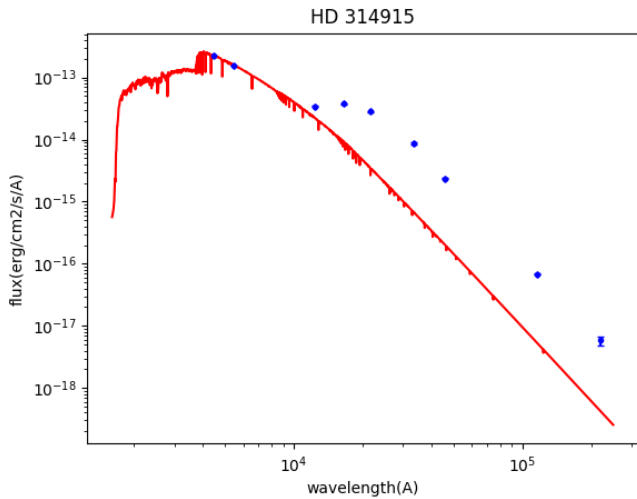


**Figure 2.** The SED of the  $\lambda$  Boo star HD 314915. Unlike the disc-hosts whose SEDs are shown in Fig. 1, this infrared excess is more consistent with a cooler stellar companion.

**Table 3.** Parameters from SED fitting, for the stars without detected infrared excesses. Asterisks in the  $T_{\text{eff}}$  column indicate the stars for which the  $V$  band rather than the  $J$  band was used for normalisation. The full machine-readable table is available online.

Obj. Name	Spectral Type	$T_{\text{eff}}$ K	$\log g$	$[\text{Fe}/\text{H}]$	$E(B-V)$ mag
BD+00 2757	F5 V: mF2gF5	6500	4.2	-0.5	0.015
CD-31 4428	A2 Van	8750 *	4.2	0.0	0.05
CD-58 3782	A3 Van	8700	4.2	-0.2	0.03
CD-60 1956	A0.5 V	9650	4.2	0.0	0.132
CD-60 1986	A2 Van	9500	4.2	0.0	0.07
CD-60 6017	A8 IV-V	7500	4.2	0.0	0.2
CD-60 6021	B7 IVn	13000 *	3.6	0.0	0.214
CPD-20 1613	A0.5 V kB9.5	9500	4.2	-0.5	0.0
CPD-58 3071	A3 Va	8500 *	4.2	0.0	0.0
CPD-58 3106	A1.5 Vn	9200	4.2	0.0	0.08
HD 100237	A1 IVs	9500	3.6	0.0	0.0
HD 100325	A1 Va	9500	4.2	0.0	0.172

mined in Sec. 3.1. Bolometric corrections, BC, were computed via grid interpolation, taking the observed  $T_{\text{eff}}$ ,  $\log g$ , and  $[\text{Fe}/\text{H}]$  from SED fitting (Sec. 3.1) and uncertainties of 250 K, 0.5 dex and 0.25 dex, respectively. These correspond to approximately 0.15 mag, 0.02 mag and 0.025 mag of uncertainty in the BC, which we combined in quadrature. We adopted a bolometric magnitude for the Sun,  $M_{\text{bol},\odot}$ , of 4.74 (Mamajek et al. 2015). Distances were calculated using Gaia DR2 parallaxes (Gaia Collaboration et al. 2018), their uncertainties, and the length-scale model of Bailer-Jones et al. (2018). To determine luminosities with uncertainties, for each star we generated 10 000 distance samples that we fed into a Monte Carlo process using equations 1 and 2, and took the median and standard deviation of the resulting distribution.

Using these luminosities together with the effective temperatures from SED fitting, we plot the  $\lambda$  Boo stars in an HR diagram in Fig. 3. The  $\lambda$  Boo stars with infrared excesses are highlighted, some of which clearly lie near the terminal-age main sequence. This confirms earlier results (Paunzen et al. 2002, 2014; Murphy & Paunzen 2017; Gray et al. 2017), that the  $\lambda$  Boo stars have a range of main-sequence ages. There is no apparent preference towards the ZAMS, even among the  $\lambda$  Boo stars with infrared excesses that are presumably attributable to discs.

## 4 CONCLUSIONS

The curation of a large and well defined sample of  $\lambda$  Boo stars is important for understanding the accretion environments and particle transport processes affecting A type stars more broadly. We have classified 308 stars on the MK system and discovered or co-discovered 24 new  $\lambda$  Boo stars, including two that require high-resolution spectroscopy for an abundance analysis to confirm their membership in the class. These represent a 17% increase in the number of known  $\lambda$  Boo stars, adding to the 64 in the Murphy et al. (2015) catalogue and the 45 in Paper I, after accounting for overlap and revised spectral types. Our revision of 11 known  $\lambda$  Boo stars revealed that one is a chemically normal rapid rotator. This one misclassified target suggests that abundance analyses would be valuable to confirm  $\lambda$  Boo stars.

**Table 4.** Breakdown of infrared excesses among the target selection groups described in Sec. 2.1. We give the number of  $\lambda$  Boo stars, and their percentage of the total group numbers; the number of stars with IR excesses, and their percentage of the measurable population (i.e. group members where we could construct and evaluate SEDs for IR excesses); and the number of  $\lambda$  Boo stars with IR excesses as a percentage of the number of  $\lambda$  Boo stars in that group.

Group	Description	Total stars	$\lambda$ Boo		IR excess		$\lambda$ Boo + IR	
			Num.	%	Num.	% of group	Num.	% of $\lambda$ Boo
0	Known $\lambda$ Boo stars	11	10	91	4	40	4	40
1	“A[0-9]*e”	20	4	20	17	85	4	100
2	“Em*/Ae*” and “A”	18	1	6	16	89	1	100
3	Photometrically metal weak	210	16	8	105	50	10	63
4	BHB stars	7	2	29	4	57	1	50
K2	K2 targets	42	1	2	11	26	1	100

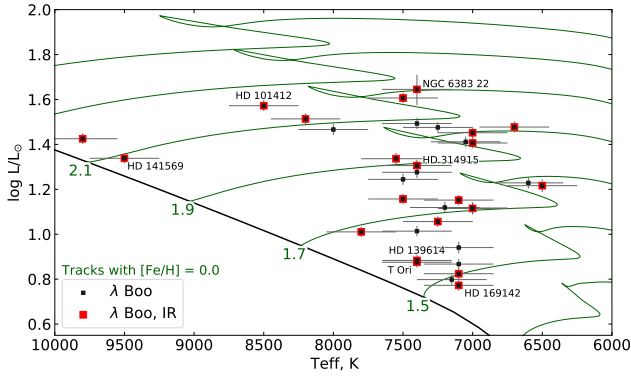


**Figure 3.** HR diagram of the 34  $\lambda$  Boo stars. The 21 stars with infrared excesses are highlighted with red boxes and the seven stars with  $> 10\sigma$  excesses are labelled (see also Fig. 1 and 2). Evolutionary tracks of solar metallicity from Murphy et al. (2019, green lines) are shown at intervals of  $0.2 M_{\odot}$ .

The fraction of field A stars that are  $\lambda$  Boo is known to be approximately 2%, whereas stars identified photometrically as being metal-weak yielded a relatively high fraction of  $\lambda$  Boo stars (8%). We estimate that roughly half of all stars with Strömgren photometry and meeting our metal-weak criteria (Sec 2.1) have now been searched for  $\lambda$  Boo stars, but with strong bias towards higher completeness in the southern hemisphere; the northern sky is comparatively underexplored, and will be the subject of future work, along with a refinement of those selection criteria to improve search efficiency. Our observations of 38 emission-line stars yielded 5 new  $\lambda$  Boo stars (13%). Emission-line stars are a relatively untapped source, since our search only used emission-line objects with known spectral types. Using further SIMBAD criteria searches, we find 1126 emission-line objects without spectral types but with the correct  $B - V$  colours ( $-0.05$  to  $0.4$ ) to be potential  $\lambda$  Boo stars. These should be high priority targets for future searches for  $\lambda$  Boo stars.

We collated fluxes in nine passbands to model the spectral energy distributions of all targets to look for infrared excesses. Unsurprisingly, infrared excesses were highly prevalent among the emission-line stars, including all those that are  $\lambda$  Boo stars. We also calculated stellar luminosities to plot the  $\lambda$  Boo stars on the HR diagram, confirming that

not all  $\lambda$  Boo stars are young: even those that have infrared excesses are found at a variety of main-sequence ages.

## ACKNOWLEDGEMENTS

The authors thank the reviewer, Frédéric Royer, whose comments improved this manuscript. This work was supported by the Australian Research Council through the award DE180101104. This research has made use of the NASA/IPAC Infrared Science Archive, which is funded by the National Aeronautics and Space Administration and operated by the California Institute of Technology. It also made use of the SIMBAD database, operated at CDS, Strasbourg, France. We used Lightkurve, a Python package for Kepler and TESS data analysis (Lightkurve Collaboration et al. 2018), and SPECTRUM for creating synthetic spectra (Gray 1999).

## DATA AVAILABILITY

Table A1, which appears in full in the appendix, is also available online. Tables 2 and 3, which contain stars with and without infrared excesses, respectively, are each shown for twelve rows in this paper and are available in full in machine-readable format online. The stellar spectra are available from the corresponding author upon reasonable request.

## REFERENCES

- Abt H. A., Morrell N. I., 1995, *ApJS*, **99**, 135
- Andrievsky S. M., et al., 2002, *A&A*, **396**, 641
- Appenzeller I., Mundt R., 1989, *A&ARv*, **1**, 291
- Bailer-Jones C. A. L., 2015, *A&A*, **575**, A35
- Bailer-Jones C. A. L., Rybizki J., Fouesneau M., Mantelet G., Andrae R., 2018, *AJ*, **156**, 58
- Baschek B., Slettebak A., 1988, *A&A*, **207**, 112
- Bessell M., Murphy S., 2012, *PASP*, **124**, 140
- Bodman E. H. L., Quillen A., 2016, *ApJ*, **819**, L34
- Boyajian T. S., et al., 2016, *MNRAS*, **457**, 3988
- Bruzzone J. S., et al., 2020, *AJ*, **159**, 53
- Carmona A., et al., 2017, *A&A*, **598**, A118
- Carney M. T., et al., 2018, *A&A*, **614**, A106
- Castelli F., Kurucz R. L., 2004, ArXiv Astrophysics e-prints,
- Chen L., et al., 2019, *ApJ*, **887**, L32
- Cheng K.-P., et al., 2016, *AJ*, **151**, 105

- Childress M. J., Vogt F. P. A., Nielsen J., Sharp R. G., 2014, *Ap&SS*, **349**, 617
- Cowley C. R., Hubrig S., Castelli F., Wolff B., 2012, *A&A*, **537**, L6
- Cugno G., et al., 2019, *A&A*, **622**, A156
- Dopita M., Hart J., McGregor P., Oates P., Bloxham G., Jones D., 2007, *Ap&SS*, **310**, 255
- Fedele D., et al., 2017, *A&A*, **600**, A72
- Ferlet R., Hobbs L. M., Madjar A. V., 1987, *A&A*, **185**, 267
- Fitzpatrick E. L., 1999, *PASP*, **111**, 63
- Folsom C. P., Bagnulo S., Wade G. A., Alecian E., Landstreet J. D., Marsden S. C., Waite I. A., 2012, *MNRAS*, **422**, 2072
- Freistetter F., Krivov A. V., Löhne T., 2007, *A&A*, **466**, 389
- Gaia Collaboration et al., 2018, *A&A*, **616**, A1
- Gratton R., et al., 2019, *A&A*, **623**, A140
- Gray R. O., 1999, SPECTRUM: A stellar spectral synthesis program (ascl:9910.002)
- Gray R. O., Corbally C. J., 1994, *AJ*, **107**, 742
- Gray R. O., Corbally C. J., 1998, *AJ*, **116**, 2530
- Gray R. O., Corbally C. J., 2002, *AJ*, **124**, 989
- Gray R. O., Corbally J. C., 2009, *Stellar Spectral Classification*. Princeton University Press
- Gray R. O., Riggs Q. S., Koen C., Murphy S. J., Newsome I. M., Corbally C. J., Cheng K.-P., Neff J. E., 2017, *AJ*, **154**, 31
- Herbig G. H., 1960, *ApJS*, **4**, 337
- Hey D. R., et al., 2019, *MNRAS*, **488**, 18
- Hillenbrand L. A., Strom S. E., Vrba F. J., Keene J., 1992, *ApJ*, **397**, 613
- Høg E., et al., 2000, *A&A*, **355**, L27
- Holweber H., Sturenburg S., 1993, in Dworetsky M. M., Castelli F., Faraggiana R., eds, *Astronomical Society of the Pacific Conference Series Vol. 44, IAU Colloq. 138: Peculiar versus Normal Phenomena in A-type and Related Stars*. p. 356
- Howell S. B., et al., 2014, *PASP*, **126**, 398
- Iliev I. K., Barzova I. S., 1995, *A&A*, **302**, 735
- Jermyn A. S., Kama M., 2018, *MNRAS*, **476**, 4418
- Joy A. H., 1945, *ApJ*, **102**, 168
- Jura M., 2015, *AJ*, **150**, 166
- Kama M., Folsom C. P., Pinilla P., 2015, *A&A*, **582**, L10
- Kamp I., Paunzen E., 2002, *MNRAS*, **335**, L45
- Kamp I., Iliev I. K., Paunzen E., Pintado O. I., Solano E., Barzova I. S., 2001, *A&A*, **375**, 899
- Karmann C., Beust H., Klinger J., 2001, *A&A*, **372**, 616
- Karmann C., Beust H., Klinger J., 2003, *A&A*, **409**, 347
- King J. R., 1994, *MNRAS*, **269**, 209
- King J. R., Patten B. M., 1992, *MNRAS*, **256**, 571
- Lagrange A.-M., et al., 2010, *Science*, **329**, 57
- Laws A. S. E., et al., 2020, *ApJ*, **888**, 7
- Lellouch E., et al., 1997, *Planet. Space Sci.*, **45**, 1203
- Lightkurve Collaboration et al., 2018, *Lightkurve: Kepler and TESS time series analysis in Python*, *Astrophysics Source Code Library* (ascl:1812.013)
- Ligi R., et al., 2018, *MNRAS*, **473**, 1774
- MacConnell D. J., Frye R. L., Bidelman W. P., Bond H. E., 1971, *PASP*, **83**, 98
- Macías E., et al., 2019, *ApJ*, **881**, 159
- Mamajek E. E., et al., 2015, preprint, ([arXiv:1510.06262](https://arxiv.org/abs/1510.06262))
- Matter A., et al., 2016, *A&A*, **586**, A11
- Mawet D., et al., 2017, *AJ*, **153**, 44
- Mendigutía I., Oudmaijer R. D., Mourard D., Muzerolle J., 2017, *MNRAS*, **464**, 1984
- Miley J. M., Panić O., Wyatt M., Kennedy G. M., 2018, *A&A*, **615**, L10
- Murphy S. J., Paunzen E., 2017, *MNRAS*, **466**, 546
- Murphy S. J., et al., 2013, *MNRAS*, **432**, 2284
- Murphy S. J., et al., 2015, *Publ. Astron. Soc. Australia*, **32**, 36
- Murphy S. J., Hey D., Van Reeth T., Bedding T. R., 2019, *MNRAS*, **485**, 2380
- Murphy S. J., Paunzen E., Bedding T. R., Walczak P., Huber D., 2020, *MNRAS*, **495**, 1888
- Nesterov V. V., Kuzmin A. V., Ashimbaeva N. T., Volchkov A. A., Röser S., Bastian U., 1995, *A&AS*, **110**, 367
- Paunzen E., 2001, *A&A*, **373**, 633
- Paunzen E., Gray R. O., 1997, *A&AS*, **126**, 407
- Paunzen E., Duffee B., Heiter U., Kuschnig R., Weiss W. W., 2001, *A&A*, **373**, 625
- Paunzen E., Iliev I. K., Kamp I., Barzova I. S., 2002, *MNRAS*, **336**, 1030
- Paunzen E., Iliev I. K., Fossati L., Heiter U., Weiss W. W., 2014, *A&A*, **567**, A67
- Schöller M., et al., 2016, *A&A*, **592**, A50
- Slettebak A., 1952, *ApJ*, **115**, 575
- Slettebak A., 1954, *ApJ*, **119**, 146
- Smith M. A., Thompson R. W., Gray R. O., Corbally C., Kamp I., 2011, arXiv e-prints, [p. arXiv:1112.3617](https://arxiv.org/abs/1112.3617)
- Snellen I. A. G., Brown A. G. A., 2018, *Nature Astronomy*, **2**, 883
- Soummer R., Brendan Hagan J., Pueyo L., Thormann A., Rajan A., Marois C., 2011, *ApJ*, **741**, 55
- Thébault P., Beust H., 2001, *A&A*, **376**, 621
- Toci C., Lodato G., Fedele D., Testi L., Pinte C., 2020, *ApJ*, **888**, L4
- Turcotte S., Charbonneau P., 1993, *ApJ*, **413**, 376
- Venn K. A., Lambert D. L., 1990, *ApJ*, **363**, 234
- Waters L. B. F. M., Trams N. R., Waelkens C., 1992, *A&A*, **262**, L37
- Wenger M., et al., 2000, *A&AS*, **143**, 9
- White J. A., Boley A. C., MacGregor M. A., Hughes A. M., Wilner D. J., 2018, *MNRAS*, **474**, 4500
- Xue M., Jiang B. W., Gao J., Liu J., Wang S., Li A., 2016, *ApJS*, **224**, 23
- Zieba S., Zwintz K., Kenworthy M. A., Kennedy G. M., 2019, *A&A*, **625**, L13
- Zuckerman B., Song I., 2012, *ApJ*, **758**, 77

This paper has been typeset from a  $\text{\LaTeX}$  file prepared by the author.

## APPENDIX A: SPECTRAL CLASSES FOR THE PROGRAM STARS



**Table A1.** Spectral classes for the program stars. We give the target group of each star (Sec. 2.1). Comments on the spectra are recorded as endnotes. Infrared excesses are denoted with ‘1’ in the final column.

Obj Name	V mag	Group	Class	Note	IR
HD 28490	9.53	3	F0 V(n) kA5mA5 ( <i>λ Boo</i> )	<sup>2</sup>	
HD 29650	9.66	3	A3 IV-Vs		1
HD 30335	9.67	2	A4 IV Sr		
HD 32725	9.52	3	F3 V Sr	<sup>3</sup>	1
HD 33901	9.52	3	A7 III		
HD 35343	10.25	1	Be3	<sup>4</sup>	1
HD 35793	9.77	3	A2 Vs		1
HD 36121	8.98	1	kA6hA8mA8 III Sr	<sup>5</sup>	
HD 36866	9.52	3	A3 Vas		1
HD 36899	9.8	3	A1 V		
HD 36955	9.58	3	A7 Vp SrEu		
HD 37091	9.82	3	A2.5 V		1
HD 37258	9.61	3	A3 V shell	<sup>6</sup>	1
HD 37357	8.85	1	A3 Van kA1		1
HD 37412	9.76	3	A2.5 Vs		1
HD 37455	9.6	3	A3 Vb		1
HD 37469	9.58	3	B9 Vp Si-Sr		1
HD 40632	9.15	1	B9 IV shell	<sup>7</sup>	1
HD 44351	8.25	1	F5 V composite	<sup>8</sup>	1
HD 46390	10.08	2	B7 IV-Ve	<sup>9</sup>	1
HD 50937	9.61	3	A2 IVn		
HD 51480	6.93	2	B3/5 Ibe	<sup>10</sup>	1
HD 55637	9.65	2	B6 IV	<sup>11</sup>	1
HD 59000	9.57	3	A8 IV/V		
HD 62752	8.11	3	B9 Vp SiEuSr	<sup>12</sup>	
HD 63524	8.8	2	B6.5 Vn		
HD 63562	9.69	3	A1 V		1
HD 66318	9.56	3	A2: IV:p SiSrCr	<sup>13</sup>	
HD 67658	9.76	3	A4 IV		
HD 68695	9.87	1	A3 Vbe kA0mA0.5	<sup>14</sup>	1
HD 75185	9.82	3	A2 IV-n.		
HD 79066	6.34	1	F1 Vn	<sup>15</sup>	
HD 80692	9.69	3	F0 V + Ae composite	<sup>16</sup>	
HD 83041	8.79	4	F1.5 V kA3mA3 <i>λ Boo</i>		
HD 83798	9.58	3	A5 IVnn		
HD 85337	9.61	3	hA9 Vn kA6mA6	<sup>17</sup>	
HD 87271	7.13	0	A8 V kA0mA0.5 <i>λ Boo</i>		1
HD 87593	9.62	3	A2 Vas		
HD 88554	9.32	3	F3 V kA6mA8 ( <i>λ Boo</i> )		1
HD 88976	6.54	3	A2 IV-V		1
HD 89234	9.79	3	A0.5 IV		1
HD 91839	8.39	3	A3 Vas (met wk A2)	<sup>18</sup>	1
HD 92251	9.81	3	A0.5 Vas		
HD 93264	9.54	3	kA1.5hA2mA3 IV-V	<sup>19</sup>	
HD 93746	9.52	3	F3 V		
HD 93925	9.24	3	A0 II-IIIp Eu		1
HD 94326	7.76	3	A6 III kA5		1
HD 95883	7.33	3	A1 Van	<sup>20</sup>	1
HD 96040	9.97	3	B9 IIIp Si		1
HD 96089	9.78	3	A1 Van		1
HD 96091	9.57	3	A0.5 Van		
HD 96157	9.82	3	A2 Van		
HD 96192	9.66	3	A3 Van kA1		1
HD 96304	9.54	3	A0.5 Van		1
HD 96341	9.53	3	A0.5 Van		1
HD 96386	9.83	3	A2 IV-V		1
HD 96430	8.49	2	B6 IV/Ve	<sup>21</sup>	1
HD 96493	8.5	3	A0.5 III shell		1

<sup>2</sup> A mild *λ Boo* star.  
<sup>3</sup> Especially clear enhancement of Sr II 4215. Might be an early Ba dwarf.  
<sup>4</sup> Strong emission in H lines and Fe II lines  
<sup>5</sup> Mild Am peculiarity.  
<sup>6</sup> Shell core in H $\beta$  and Fe II 4233.

<sup>7</sup> Strong metallic-line spectrum, similar to F0 III. The Fe II 4233 line is strong and the hydrogen line cores are deep.  
<sup>8</sup> The K line is broad and shallow, while metal lines are of mixed strengths.  
<sup>9</sup> Emission reversal in H $\beta$ . H $\gamma$  and H $\delta$  partially filled with emission.  
<sup>10</sup> P Cygni profile  
<sup>11</sup> Classified in Simbad as emission line Ap Si. No sign of emission or increased abundance of Si.  
<sup>12</sup> Very peculiar.  
<sup>13</sup> Very peculiar. Temperature type very uncertain. H lines do not fit well at any spectral type.  
<sup>14</sup> Emission in the core of H $\beta$ . Mg II 4481 is normal. Not a *λ Boo* star.  
<sup>15</sup> Rapid rotation gives the impression of metal weakness unless comparing against high  $v \sin i$  standards.  
<sup>16</sup> H $\beta$  has broad wings and a deep narrow core, suggesting shell, emission, or composite. K-line about A1. Hy is F0 V. Note that Simbad has this as an eclipsing binary.  
<sup>17</sup> More rapidly rotating than the Vn standards. Metal weak even after considering rotation.  
<sup>18</sup> Not a *λ Boo* star.  
<sup>19</sup> A mild Am star.  
<sup>20</sup> Shallow H cores.  
<sup>21</sup> Emission in core of H $\beta$ , possibly causing other H lines to be shallower.  
<sup>22</sup> Not an Am star since the K line is strong, too.  
<sup>23</sup> A mild *λ Boo* star, with fluted H $\gamma$  lines  
<sup>24</sup> A  $\rho$  Pup star.  
<sup>25</sup> Mild Am, with anomalous luminosity effect.  
<sup>26</sup> Marginal Am star. Anomalous luminosity effect evident.  
<sup>27</sup> Metal weak overall, but less so in K line. Weakness of Ca I 4226 and the difference between the K and m types suggest this is not a *λ Boo* star, despite weak Mg II 4481 line. May be composite.  
<sup>28</sup> Slight emission notch in H $\beta$ . A mild *λ Boo* star.  
<sup>29</sup> Not a *λ Boo* star – Mg II 4481 is not additionally weak. Fe I 4046 is peculiarly strong in absorption.  
<sup>30</sup> H lines fit best at A1 V, and are too narrow for A2. A2 IV is not as good a fit as A1 V. Metal lines and K line are strong for A1, being  $\sim$ A2.  
<sup>31</sup> Not a *λ Boo* star, just marginally metal weak.  
<sup>32</sup> Very peculiar spectrum. Very weak H lines, which can be approximately fitted by a B7 supergiant, or a mid-late F supergiant. In the case of the latter, the star is profoundly metal weak. Most likely a pop II star, possibly a high-latitude F supergiant, although the spectrum is peculiar even for that class.  
<sup>33</sup> Very chemically peculiar star. H lines much deeper than A0 III, but wings agree.  
<sup>34</sup> Luminosity criteria (e.g.  $\lambda\lambda 4172-8$ ) do not agree with the hydrogen line type of A3 II, but otherwise a good match.  
<sup>35</sup> Not a *λ Boo* star, maybe pop II or composite A + F.  
<sup>36</sup> Definite *λ Boo* star. Mg II 4481 is extremely weak.  
<sup>37</sup> Highly peculiar star. H lines, especially. H $\beta$  is deeper than the standard, may be shell absorption.  
<sup>38</sup> Slightly weak K line (A2).  
<sup>39</sup> Excellent match to standard, HR 2324.  
<sup>40</sup> Extreme *λ Boo* star.  
<sup>41</sup> H lines are truly halfway between A0 Van and A1 Van. Metal lines are consistent with this.

**Table A1. continued.** Spectral classes for the program stars.

Obj Name	V mag	Group	Class	Note	IR
HD 96667	9.58	3	A1 Van		
HD 96773	9.69	3	A1 Van		1
HD 97230	8.62	K2	A7 IV (met str F2)	22	
HD 97340	8.15	K2	A9 V mA6		
HD 97373	8.67	K2	A4 IVn		
HD 97528	7.31	3	A2 IIIe shell		1
HD 97678	8.67	K2	F2 Vs		
HD 97859	9.35	K2	B8 IVp Si		
HD 97891	8.33	K2	F5.5 V		
HD 97916	9.2	K2	F5.5 V gF2.5kF2:mA6		1
HD 97991	7.41	K2	B1 V		1
HD 98069	8.16	K2	A9 V kA2mA2 ( $\lambda$ Boo)	23	1
HD 98563	8.27	K2	F7 V		
HD 98575	9.12	K2	kA5hA9mF3 III	24	
HD 98632	7.57	K2	F4 Vs mF1		1
HD 98645	8.8	K2	F1 Vs		
HD 98686	7.65	K2	A8 Vnn		
HD 98711	8.07	K2	F6 IV-V		
HD 98914	8.08	K2	F5.5 V		
HD 99210	6.74	K2	kA8hA9mF2 III:	25	1
HD 99304	8.58	K2	F5 IV		
HD 99776	9.18	K2	A2.5 Vas		
HD 100237	7.34	K2	A1 IVs		
HD 100325	9.28	3	A1 Va		
HD 100380	6.78	3	A4 IVs		1
HD 100415	9.06	K2	kA6hA8mF1 (IV-III)	26	
HD 100417	8.03	K2	A1 Vas		
HD 100453	7.79	1	F1 Vn		1
HD 100630	7.88	K2	A1.5 Va		
HD 100762	9.32	K2	F4 Vs		
HD 100995	8.09	K2	F4.5 V		
HD 101196	8.5	K2	F4 Vs		
HD 101268	9.55	3	F1 Vs kA8mA6	27	
HD 101412	9.29	3	A3 V(e) kA0.5mA0.5 ( $\lambda$ Boo)	28	1
HD 101784	7.54	K2	A0 Vas		
HD 101846	7.87	K2	A4 Vs		1
HD 101969	7.54	K2	F4 V		1
HD 102059	7.76	K2	F4 Vs		1
HD 102083	8.58	K2	F0 V mA7		
HD 102284	8.54	K2	F3 IVs		1
HD 102331	7.57	K2	F4 Vs		
HD 102332	8.51	K2	F4 IVs		1
HD 102431	8.95	K2	F5.5 V		
HD 102519	8.66	3	A1 IVn		1
HD 102541	7.94	3	hA9 V kA5mA6	29	
HD 102731	8.49	K2	A6 IVs		
HD 103547	9.38	K2	F1 Vs mF2.5		1
HD 103631	8.53	K2	F8 IV		
HD 103695	8.52	K2	A6 V		
HD 104367	7.78	K2	F6 IV		
HD 104446	9.05	3	A1 IVs		1
HD 104624	9.13	K2	A4 V		
HD 104650	9.78	3	A1 Vas mA2	30	1
HD 104697	9.46	3	A1 Va		1
HD 105015	8.64	3	A1 Vas		
HD 105194	9.32	3	hA0.5 Van kB9.5mA0	31	
HD 105209	8.67	3	A2 IVn		1
HD 105232	8.66	3	A2 Vs		
HD 105649	9.83	3	A2 IV-V		1
HD 106373	8.9	4	F5: Ia: kA3mA3	32	1
HD 106961	8.93	3	A0 Vann		
HD 107049	9.36	3	A0 IV+		1

**Table A1. continued.** Spectral classes for the program stars.

Obj Name	V mag	Group	Class	Note	IR
HD 107096	9.37	3	A0: III:p Eu	33	1
HD 107127	9.57	3	A1 IV		
HD 107233	7.36	0	F0 V kA3mA2 $\lambda$ Boo		
HD 107369	9.6	4	A3 IIp	34	1
HD 107483	9.3	3	A1 IV-III		
HD 107878	9.71	3	A9 V mA2	35	
HD 108417	8.98	3	A2 V		1
HD 108889	8.86	3	A1 IVs		1
HD 108925	6.45	3	A3 IVn		
HD 109065	8.16	3	A1 IVn		
HD 109183	9.1	3	A1 Va+s		
HD 109435	8.99	3	A7 IV		1
HD 109443	9.25	3	F3 V kF1mF1		
HD 109517	8.77	3	kA0hA0mA1 IV-V		1
HD 109738	8.3	0	hA9 Vn kA0mA0 $\lambda$ Boo	36	
HD 109791	9.75	3	A0 II-IIIp SrSiEu shell?	37	
HD 109800	8.84	3	A1 IV+s		1
HD 109808	7.13	3	A3 V	38	
HD 109886	8.61	3	A1 Van	39	
HD 110640	9.0	3	A2 Vas		
HD 111105	7.25	3	A3 IVn		1
HD 111164	6.09	0	A4 V(n)		
HD 111209	9.62	3	A4 Vn		1
HD 111438	9.18	3	A1.5 Vas		
HD 111439	8.87	3	A3 IV-Vs		
HD 111786	6.14	0	F0 Vs kA1mA1 $\lambda$ Boo	40	1
HD 112938	8.16	3	A2 IV-V		1
HD 113199	8.81	3	A2 V		1
HD 113660	9.32	3	A6 IVs		1
HD 113807	7.56	3	A2 Vas		
HD 114477	8.4	3	A1.5 IVs		
HD 114738	7.81	3	A1 IV-V		
HD 114836	8.74	3	A0.5 Van	41	
HD 115843	9.34	3	A1 IVs		
HD 116137	9.09	3	B9.5 Van		
HD 119561	9.79	3	A1 Van		
HD 119896	8.22	3	F5 Vs kA5mA5 $\lambda$ Boo		1
HD 120122	9.11	3	F1 Vs kA6mA6 ( $\lambda$ Boo)		
HD 120873	9.36	3	A1 Van		
HD 121875	9.26	3	A2 IV-Vn		
HD 122264	9.59	3	A0 IIIp EuSr		
HD 122757	8.8	3	A3 Va+s		
HD 123960	9.75	3	B9 IIIp Si		1
HD 124228	7.86	3	A3 IV+s		
HD 124878	9.54	3	B8 V He-wk + A	42	
HD 126164	9.41	3	A0 Vbn		
HD 126627	9.0	3	F1 V kA5mA5 ( $\lambda$ Boo)		1
HD 127659	9.31	3	F2 V kA3mA4 $\lambda$ Boo		1
HD 128336	9.08	3	F4 V kA2mA2 $\lambda$ Boo?	43	
HD 129389	9.68	3	A0 Van		1
HD 130156	9.35	4	kA6hF1mF3 (II)	44	
HD 133800	6.4	3	A6 V kA0.5mA0.5 $\lambda$ Boo		1
HD 134685	7.67	3	A1 V		1
HD 135284	9.23	3	A3 IV+s		
HD 136463	9.54	3	F1 V kF1mA7	45	
HD 137128	7.1	3	A3 IV-V		
HD 138274	8.8	3	A1 IVs		
HD 138753	8.54	3	A0.5 Van		
HD 138921	9.72	3	A9 Vn kA4mA4 $\lambda$ Boo	46	
HD 139612	9.27	3	A0 IVs		
HD 139614	8.24	1	A9 Vs(e) kA5mA7 ( $\lambda$ Boo)	47	1
HD 139787	9.77	3	A4 V		

<sup>42</sup> Composite spectrum.<sup>43</sup> Late  $\lambda$  Boo candidate. Needs abundance analysis to decide.<sup>44</sup> H lines are not consistent, F0/3.<sup>45</sup> Difference in K and M type argues against a  $\lambda$  Boo classification.<sup>46</sup> Hydrogen line is at A9, when comparing to the A9 Vn standard.<sup>47</sup> Slight emission notch in H $\beta$ . Mild  $\lambda$  Boo star - slight additional weakness in the Mg II 4481 line.<sup>48</sup> Great match to the A5 IV standard,  $\beta$  Tri, except for the Ca I 4226 line, which is much stronger than in the standard.<sup>49</sup> Mild Am.<sup>50</sup> The Mg II 4481 line is weak, but this is not a  $\lambda$  Boo star, since the K line is normal.<sup>51</sup> Slightly shallow H cores.

**Table A1. continued.** Spectral classes for the program stars.

Obj Name	V mag	Group	Class	Note	IR
HD 140734	9.55	3	A5 IV	48	
HD 141063	6.98	3	kA2hA3mA5 Va+	49	
HD 141403	9.03	3	A1 Vbs		1
HD 141442	8.74	3	A1 Va		
HD 141444	8.94	3	A0 Va	50	
HD 141569	7.12	1	A1 Vn kB9mB9 $\lambda$ Boo		1
HD 141576	9.04	3	A0.5 Vas		
HD 141905	8.3	3	A2 Va+n		
HD 142404	9.14	3	A1.5 Vas	51	
HD 142524	9.59	3	A1 Van		
HD 142666	8.82	1	F0 V shell	52	1
HD 142703	6.12	0	F1 Vs kA1.5mA1.5 $\lambda$ Boo		
HD 142705	7.74	3	A1 Vann		1
HD 142931	9.79	3	A1.5 Vas		
HD 142994	7.17	0	hF2 V kA5mA5 ( $\lambda$ Boo)		1
HD 143511	8.31	3	A1 Vas	53	
HD 143567	7.19	3	B9 Van	54	
HD 143600	7.33	3	B9 Vn	55	1
HD 143715	7.14	3	A1.5 IVs	56	1
HD 143747	8.4	3	A1 IVn		
HD 143822	9.39	3	A1 Vbn		
HD 143956	7.77	3	B9 Van		1
HD 144254	7.78	3	A1 Van kA0.5		1
HD 144273	7.54	3	B9 Vn		1
HD 144569	7.9	3	A1 Vas mA0.5	57	1
HD 144586	7.81	3	A1 IV-V kB9	58	1
HD 144668	7.05	1	A9 V shell	59	1
HD 144925	7.78	3	A0 Vn	60	1
HD 144981	8.04	3	A0.5 Vn		1
HD 145188	7.06	3	B9.5 Vb		1
HD 145631	7.6	3	B9 Vann		1
HD 146706	7.55	3	B9 Van		1
HD 147010	7.4	3	B8: Vp SrTiSiEu		1
HD 147046	7.8	3	A2 IVn	61	1
HD 148036	9.62	3	F0.5 Vn kA6mA6	62	
HD 148534	9.02	3	A2 Vas		
HD 148563	8.72	3	A2 Va		1
HD 148638	7.9	3	A2 IV-Vn		1
HD 149130	8.48	3	F1 Vp Sr	63	1
HD 149151	8.12	3	A0 IV-V SrSi		
HD 150035	8.71	3	A2 IVp SrCrEu		1
HD 150193	8.79	1	A3 Va(e)	64	1
HD 151873	9.1	2	B9 III shell	65	1
HD 153747	7.42	0	A6 Vn kA0mA0 $\lambda$ Boo	66	
HD 153948	9.54	3	B9 IVp SiSrCrEu		1
HD 154153	6.18	3	F1.5 Vs kA4mA4 $\lambda$ Boo		1
HD 154751	8.96	3	A3 IV		
HD 154951	8.78	3	F2 V kA6mA6 (( $\lambda$ Boo))	67	
HD 155127	8.38	3	kA0hA5mF0 II		
HD 155397	9.53	3	F2 Vs		1
HD 156300	8.65	3	A1: IIIp EuCr(Sr)		
HD 156974	9.39	3	A0.5 IVs		1
HD 157170	7.97	3	kA0hA1mA2 V	68	
HD 157184	9.48	3	A1 V		
HD 157389	9.98	3	B9 IV-Vn		1
HD 158681	8.22	3	B6 IV:	69	
HD 158830	8.97	3	A1 IV-V (shell)	70	1
HD 159014	9.64	2	B7 IV-V(e)	71	1
HD 160461	7.51	3	A1.5 IVn		
HD 161576	9.26	3	A4 Vn		
HD 161595	9.17	3	A1 Vas		1
HD 162220	6.66	3	B9 IVn		1
HD 163296	6.85	1	A3 Vae kA1mA1	72	1

- 52 Very deep H-line cores.  
53 Great match to the standard star.  
54 Very slight weakness in the Mg II 4481 line, and the Ca II K line is a little weak, but B9 is too early to claim weak metal lines.  
55 Slightly shallow H cores.  
56 Weak H cores.  
57 Metal lines (except K line) are slightly weak. Not a  $\lambda$  Boo star.  
58 H lines well-matched at A1 IV-V, not at A0 IV-V. But trace He suggests A0. Could alternatively be a low-luminosity late-B star, e.g. B9.5 Vbn. The Mg II 4481 line is weak, but rotation is very rapid, so probably not a  $\lambda$  Boo star.  
59 Very deep H-line cores.  
60 Slightly shallow H cores.  
61 Excellent match, except for slightly shallow H cores.  
62 Not a  $\lambda$  Boo star.  
63 Sr lines are strong. The Mg II 4481 is slightly weak. Not a  $\lambda$  Boo star.  
64 Slight emission notch in H $\beta$ .  
65 Classical shell star. Strong lines of Fe II, deep absorption cores in H lines, emission notch in H $\beta$ .  
66 An extreme  $\lambda$  Boo star.  
67 A very marginal  $\lambda$  Boo star.  
68 Possibly a very mild and early Am star.  
69 H cores are too deep for B5 V, and wings are too deep for B5 III. He lines are slightly weaker than B5, so B6 IV is the best match.  
70 Fe II 4232 is slightly enhanced, as well as the one line of the Fe II (42) multiplet that is visible in this spectrum, suggesting a shell. H line cores are also quite deep, more so than can be explained by slow rotation.  
71 Emission in core of H $\beta$ , infilling in H $\gamma$ . He I slightly weak for B7, so may be B7.5.  
72 Not a  $\lambda$  Boo star, since the Mg II 4481 line is normal.  
73 Intermediate between the A9 Vn standard, 44 Cet, and the F0 V standard, HD23585, broadened to  $v \sin i = 150 \text{ km s}^{-1}$ .  
74 Classic  $\lambda$  Boo star.  
75 Cores are too narrow for an earlier giant (e.g. A4 III-IV). The Mg II 4481 line is weak.  
76 The Ca I 4226 line is strong while Mg II 4481 is weak. A mild  $\lambda$  Boo star.  
77 The Mg II 4481 line is rather weak, but not much difference between h and km types. A mild  $\lambda$  Boo star. This target was observed twice and each spectrum was classified independently, arriving at similar classifications. The Sr II 4077 line is unusually strong in one of the spectra, but the Sr II 4215 line is normal.  
78 Metal weak, not clearly  $\lambda$  Boo in nature.  
79 Could serve as spectral standard for B9 Vbs.  
80 Blue horizontal branch star? Mg II 4481 is weak, although not with respect to A5 II line ratios.  
81 Emission in H $\beta$  (in an inverted 'w' shape), strong absorption in Si 4128-30 and the Ca II K line.  
82 Emission partially fills H $\beta$ .  
83 Slightly noisy spectrum.  
84 Possibly a mild Am star, with the K line weaker than the metals, but also definitely a rapid rotator.  
85 Emission partially fills H $\beta$ .  
86 Very rapid rotation. Even so, the Mg II 4481 line is weak.  
87 Slightly shallow H cores.

**Table A1. continued.** Spectral classes for the program stars.

Obj Name	V mag	Group	Class	Note	IR
HD 163921	9.52	3	A9.5 Vn	<a href="#">73</a>	1
HD 168740	6.12	0	A9 Vs kA2mA2 $\lambda$ Boo	<a href="#">74</a>	1
HD 168947	8.11	0	A9 Vs kA3mA4 ( $\lambda$ Boo)	<a href="#">75</a>	
HD 169142	8.16	3	F1 Vs kA4mA5 ( $\lambda$ Boo)	<a href="#">76</a>	1
HD 169346	9.27	3	A8 V kA6mA6 ( $\lambda$ Boo)	<a href="#">77</a>	
HD 171013	8.6	3	F2 Vs kA8mA7	<a href="#">78</a>	1
HD 176386	7.21	3	B9 Vbs	<a href="#">79</a>	1
HD 176387	8.94	4	A5 II-III kA0mA0	<a href="#">80</a>	1
HD 184779	8.9	0	F0 V kA5mA6 ( $\lambda$ Boo)		
HD 188230	8.18	3	A0 Vbn		
HD 261520	10.11	1	B5 II-IIIe shell	<a href="#">81</a>	1
HD 288947A	11.13	2	B7 IV-Ve	<a href="#">82</a>	1
HD 290469	9.87	3	A4 Vs		1
HD 290470	9.77	3	A2.5 V		1
HD 290516	9.51	3	B9 Vbn		
HD 290666	10.03	3	A0 Van		1
HD 290684	9.7	3	A2 V kA1		
HD 292895	11.16	2	B8 Vn	<a href="#">83</a>	1
HD 294054	9.6	3	kA0hA0mA1 Vbn	<a href="#">84</a>	
HD 294103	9.7	3	A1 Van		1
HD 294253	9.67	3	A0 Va kA8.5mB9 ( $\lambda$ Boo)		1
HD 296192	10.21	2	B7.5 IV-Ve	<a href="#">85</a>	1
HD 304838	9.87	3	B8.5 V		
HD 307860	8.28	3	B8.5 Vnn		1
HD 308889	10.64	2	B6 V(e)		1
HD 309344	10.85	2	A4 III-IV		1
HD 314915	11.31	2	A9 Vn kA5mA5 ( $\lambda$ Boo)	<a href="#">86</a>	1
HD 318093	9.71	3	A0 Va+s		1
HD 318099	9.86	3	A0 Van	<a href="#">87</a>	
HD 318127	9.82	3	A1 IVn		1
HD 320460	10.63	2	B5 IIIe	<a href="#">88</a>	1
HD 320765	8.73	3	A1 V		1
HD 322663	9.77	3	A1 IVn		1
BD+00 2757	10.64	K2	F5 V: mF2gF5		
BD-02 2182	9.71	2	B2 Vn		1
BD-08 1151	9.82	3	A2 IV-V		1
BD-11 1239	9.7	3	A7 V kA3mA3 (( $\lambda$ Boo))		1
BD-11 1762	10.05	3	B2 IV-Vn		1
BD-15 1548	9.88	1	B7 IIIe He-wk		1
BD-15 4515	9.97	4	F2 V kA4mA6 $\lambda$ Boo		1
CD-31 4428	9.86	3	A2 Van		
CD-37 3833	9.92	3	A2 Vn kA0		1
CD-48 3541	9.67	3	A2 Vn kA0mA1	<a href="#">89</a>	1
CD-55 2595	10.31	2	B1 Ve	<a href="#">90</a>	1
CD-58 3782	9.79	3	A3 Van		
CD-59 1764	9.65	3	A0.5 V		1
CD-60 1932	9.93	3	A0 Vnn	<a href="#">91</a>	1
CD-60 1956	9.65	3	A0.5 V		
CD-60 1986	9.57	3	A2 Van		
CD-60 4157	9.38	3	A1 Van		1
CD-60 6017	9.63	3	A8 IV-V		
CD-60 6021	9.73	3	B7 IVn		
CPD-20 1613	10.0	3	A0.5 V kA9.5		
CPD-58 3071	9.85	3	A3 Va		
CPD-58 3106	9.76	3	A1.5 Vn		
CPD-58 3138	9.73	3	A1.5 Vs		1
IK Hya	10.23	4	B7 II kA3mA3	<a href="#">92</a>	
KK Oph	10.99	1	A9:e	<a href="#">93</a>	1
NGC 6383 22	12.49	1	F1 V(e) kA6mA6 $\lambda$ Boo?	<a href="#">94</a>	1
T Ori	11.25	1	A8 Vne kA1mA2 $\lambda$ Boo	<a href="#">95</a>	1
V1012 Ori		1	F3 V kA5n composite	<a href="#">96</a>	
V748 Cen	11.93	2	A0e	<a href="#">97</a>	1
V Lep	9.71	3	F0.5 V(n) kA8mA9	<a href="#">98</a>	1

<sup>88</sup> Emission core in H $\beta$ , infilling in H $\gamma$ , and possibly H $\delta$ .<sup>89</sup> Not a  $\lambda$  Boo star, just slightly metal weak<sup>90</sup> Spectrum contaminated, H $\beta$  partially filled with emission.<sup>91</sup> Rotating more rapidly than the high  $v \sin i$  A0 V standard.<sup>92</sup> Known RRLyr variable.<sup>93</sup> Emission in H $\beta$ , Ca II K and H, and some other metallic lines.

Probably pre main sequence, or possibly an RS CVn variable. This is KK Oph, a known Herbig Ae/Be star.

<sup>94</sup> The Ca II K line has a peculiar profile (broad but shallow). Enhanced G-band absorption suggests this is a composite spectrum. The Mg II 4481 line is slightly weak. A high-resolution spectrum is needed to determine if this is a mild  $\lambda$  Boo star or a composite instead.

<sup>95</sup> H $\beta$  in emission, emission core in H $\gamma$ .

<sup>96</sup> Might be a triple system: both line veiling, indicating a hotter companion, and a strong G-band red edge, indicating a cooler companion, are evident.

<sup>97</sup> Most lines are in emission, H $\beta$  strongly so. SpT from Ca II K line.

<sup>98</sup> Not a  $\lambda$  Boo star, just slightly metal weak.